# STUDY ON LOW CYCLE FATIGUE OF STRUCTURAL FRAMES DUE TO RANDOMLY VARYING LOAD

by

Kōji MIZUHATA,(I) Yoshihisa GYŌTEN,(II) Haruyuki KITAMURA(III)

## SYNOPSIS

In this study, both constant and random displacement amplitude low cycle fatigue tests were conducted for the steel frames used in tall residential buildings, and after formulating the restoring force characteristics, realistic earthquake response analyses were done for 8∿28 storied buildings, and then several random fatigue theories were applied to their results. It has been concluded that the frame attains to failure by propagation of crack initiated at the weld of the flange of the girder end, and that the maximum ductility factor can not be a sure measure compared with the damage factor.

## INTRODUCTION

This paper consists of two parts. In the first part, for the purpose of clarifying the low cycle fatigue and the restoring force characteristics of steel frames to be used in tall residential buildings, their constant displacement amplitude fatigue tests and randomly varying displacement fatigue tests are conducted. In the second part, after formulating the restoring force characteristics, realistic earthquake response analyses are done, and by applying the random fatigue theories to their results, seismic safety of the structure can be evaluated more reasonably.

## PART I EXPERIMENTAL STUDY

### Test Frame

Test frames were made based on a quarter size model of the frame selected in the middle height of an existing residential building of steel framed reinforced concrete. Steel used in its main members is SM50. The test frame is shown in Fig.1. Its columns and girders are of H-150•75•7•10 section, whose flange was cut off by gas and ground from H-150•150•7•10. Girders are welded by the K-type with columns, whose web makes the panel zone together with two plates. The right-up corner and the bottom parts of the model in Fig.1 are worked up so as to be connected with the hydraulic cylinder and the supports, respectively. Eight steel frames were tested and their names are according to the following notation:

Ex: [S] — [A] — [1]

[Steel] [A: Static, B: Constant Amplitude Fatigue, C: Random Fatigue] [Test No]

The average results of the material tests of six steel specimens were as Yield stress: 4.45t/cm$^2$, Tensile strength: 5.82t/cm$^2$, Ductility: 19.44%.

### Plan and Method of Experiment

In this study, the monotonic loading static test, the deflection controlled constant amplitude fatigue test, and the random load fatigue test were conducted. The testing machine used in this experiment belongs to the structural dynamics laboratory at Kobe University and utilizes the closed-loop electro-hydraulic servomechanism. The test frame was loaded horizontally at the right-up corner by the hydraulic cylinder through the load cell and the hook and the shackle between them. In the static test, the load was applied in the following four stages as shown in Fig.2: (1) Reversals in the elastic range, (2) Hysteresis in the small plastic displacement of 12mm, (3) Hysteresis in the large plastic displacement of 37mm, (4) The last stage. In the constant amplitude fatigue test, four deflection controlled constant amplitude tests were conducted for three amplitudes of small, middle and

(I),(II),(III): Assoc. Prof., Prof. and Former Grad. Stud. at Kobe Univ.

large levels ranging 1/64.6∿1/22.8 to obtain the $\Delta\delta$-$N_f$ relationship (where $\Delta\delta$ is the interfloor displacement amplitude and $N_f$ is the number of cycles to failure), the load-displacement hysteresis curve, the dynamic strain distribution, and the mode of failure, as shown in Table 2. In the random fatigue test, three tests with different maximum amplitudes were conducted to obtain the relationship between the rms. value of amplitude and the number of cycles to failure and to compare the fatigue damage factor based on the different cumulative damage theories. As the input signal, the sinusoidal wave and the white noise were generated by low frequency wave and white noise generators, respectively, and recorded by a data recorder, which was speeded down in replaying in the experiment. The loading rate was chosen the order of the fundamental period of a high-rise building. In all the constant amplitude fatigue test frames other than S-B-4, the cyclic rate was 4.4sec/cycle, while in the S-B-4, the cyclic rate slowed down to 10sec/cycle. The actual frequency band used in the random fatigue test was DC∿0.125Hz. The loading was ceased when the test frame was broken, but the failure on the $\Delta\delta$-$N_f$ curve is defined the crack initiation in this paper, instead of reduction of load in Bibl.(1). The horizontal load applied was measured by the load cell set up between the test frame and the hydraulic cylinder and recorded continuously by a data recorder, a pen writing oscillograph and a XY-recorder. The horizontal displacements, L-1 and L-2 (or D-2), on the girders and the vertical displacements, D-9 and D-12, at the supports as shown in Fig.1 were measured by the displacement meter of strain gage type, whose output was also recorded continuously. In the static test, displacements at more positions than in the dynamic test were measured by dial gages. On the web plates in the panel zones and at the end of the girders and the columns, rosette strain gages were adhered. On the flange plates at the end of the girders and the columns and on the web plates at the center of the member, uniaxial strain gages were adhered. In the static test, output of all the strain gages were read out, but in the dynamic constant amplitude test, selected 28 outputs were recorded continuously.

Experimental Results and Discussions

(1) Results and Discussions of the Static Test: Experimental results of the static test, S-A-1, are shown in Table 1. Relationship between the horizontal load and the interfloor displacement is shown in Fig.2. This curve has been drawn by plotting the direct readings of the load cell vs. the interfloor displacement calculated by the formula

$$(L\text{-}1)-(L\text{-}2)-\tfrac{1}{2}[(D\text{-}9)-(D\text{-}12)] = \text{Interfloor Displacement} \qquad (1)$$

The $P=k\delta^n$ type equations, where P is the load and $\delta$ is the interfloor displacement, have been obtained by replotting the above relationship on the log-log graph paper. The experimental results of the load at the flange yield and the initial rigidity agree well with the analytical results of the rigid frame. Regarding the strain distribution, the strain in the panel zone is the largest. As for the mode of fracture, the frame reaches the last stage by lateral buckling of the upper girder.

(2) Results and Discussions of the Dynamic Constant Amplitude Fatigue Test: Comparative results of four dynamic constant amplitude fatigue tests, S-B-1, S-B-2, S-B-3, S-B-4 are shown in Table 2 and as follows:

(i) Typical hysteresis loops of the horizontal load vs. the interfloor displacement for each test frames are shown in Fig.3. These loops have been drawn by plotting continuously the outputs of the load cell vs. the interfloor displacement calculated by Formula (1). These loops are of spindle shape which consists of a linear part and one or two curving parts of $P=k\delta^n$ type. Constants k and n have been obtained by replotting the above loops on the log-log graph paper. In Table 2, the n values are shown together with

their available range. These hysteresis loops were stable until initial crack except first few cycles.

(ii) The log-log relationships between the number of cycles and the load range are shown in Fig.5. The number of cycles to failure $N_f$ is defined the number of cycles until initiation of visible crack. By plotting the number of cycles to failure $N_f$ vs. the interfloor displacement range $\Delta\delta$ on the log-log paper as shown in Fig.4, one obtains

$$\Delta\delta \cdot N_f^{0.12} = 3.64 \quad \text{for the elastic range,} \tag{2}$$

$$\Delta\delta^e \cdot N_f^{0.74} = 12.8 \quad \text{for the plastic range, and} \tag{3}$$

$$\Delta\delta^p \cdot N_f^{0.34} = 11.6 \tag{4}$$

$$\left.\begin{aligned} \Delta\delta &= 3.64N_f^{-0.12} + 12.8N_f^{-0.74} \end{aligned}\right\} \quad \text{for the total range} \tag{5}$$

where $\Delta\delta$ is measured by cm. The exponent 0.34 of $N_f$ for the total range is very similar to that of the results $\Delta\varepsilon \cdot N_f^{0.346} = 0.0624$ for the tension-compression low cycle fatigue test of thin walled cylinders of SS41 steel conducted by the authors[2] before.

(iii) The displacement of 7mm at the flange yield was used for calculating the ductility factor. The equivalent stiffness is defined the slope of the line connected with both extreme values of load and displacement. The equivalent viscous damping factor was calculated by the formula

$$h_e = \frac{1}{2\pi} \cdot \frac{\text{Area inside the hysteresis loop}}{\text{Area of triangular surrounded by equivalent stiffness and abscissa}} \tag{6}$$

(iv) Mode of fracture in all the dynamic constant amplitude fatigue test was such that the last stage is attained by propagation of cracks initiated at the weld of the flange of the girder end and the stiffener of the panel zone mostly at the right-up corner of the test frame.

(v) Distribution of the dynamic strain in the initial cycle in the test frame lasted until crack initiation, but after that it changed greatly. Dynamic strain was larger in the panel zone and on the flange at the girder end and this coincides with the mode of fracture stated in the previous paragraph.

(3) Results and Discussions of the Randomly Varying Load Fatigue Test:

(i) In the random fatigue tests, also, the last stage was attained by crack propagation at the weld of the girder end like as in the constant amplitude fatigue tests and, hence, failure was determined by taking into account both the visible crack initiation and variation of the equivalent rigidity reduction ratio with time in Fig.6, which is defined by the following formula:

$$\text{Equivalent Rigidity Reduction Ratio} = (\overline{K}_{eq} - K_{eq})/\overline{K}_{eq} \tag{7}$$

where $\overline{K}_{eq}$ is the standard equivalent rigidity obtained from the standard restoring force characteristics.

(ii) The log-log relationships between the number of cycles to failure by means of the following six count methods,[3] and the rms. values $\overline{\Delta\delta}$ of interfloor displacement amplitude shown in Table 3 have been plotted in Fig.7: (a) Peak C. M., (b) All Peaks C. M., (c) Range C. M., (d) Range-pair C. M., (e) Range-mean C. M., (f) Full Wave C. M.. In Fig.7, it is recognized that the slope of $\overline{\Delta\delta}$-$N_f$ curve is the same as that in the constant amplitude test.

(iii) The damage factor, $\Sigma(n_i/N_i)$, where $N_i$ is the number of cycles to failure at the displacement range $\Delta\delta_i$ and $n_i$ is the number of cycles at $\Delta\delta_i$, was calculated based on $\Delta\delta$-$N_f$ curve of the constant amplitude test by means of the following four cumulative damage theories: (a) Sachs-Weiss,[4] (b) Yao-Munse's,[5] (c) Ohji-Miller's,[6] and (d) Morrow-Landgraf's,[7] and the results have been shown in Table 4, from which it is mentioned that scatter of the data is pretty large and that the damage factor is smaller than unity. The scatter may be caused partly by uncertainty of finding the crack initiation.

## PART II EVALUATION OF EARTHQUAKE RESPONSE FROM THE VIEW POINT OF FATIGUE

### Formulation of Restoring Force Characteristics

The restoring force characteristics in the above experiments have been

expressed to be the following two types of formulas and shown in Fig.8:

(i) Power Function Type:
$$P=k_0\delta \quad \text{for } \delta\leq\delta_Y \tag{8}$$
$$P=k_0\delta+k_1(\delta-\delta_Y)^n \quad \text{for } \delta_Y\leq\delta\leq\delta_D \tag{9}$$
$$P=k_2(\delta-\delta_D)+P_D \quad \text{for } \delta\geq\delta_D \tag{10}$$

(ii) Bilinear Type:
$$P=k_0\delta \quad \text{for } \delta\leq\delta_Y \tag{11}$$
$$P=n'k_0(\delta-\delta_Y)+P_Y \quad \text{for } \delta\geq\delta_Y \tag{12}$$

where $n=1.371$, $\alpha_D=2.03$, $\mu_D=4.5$, $\delta_D=\mu_D\delta_Y=4.5\delta_Y$, $P_D=\alpha_D P_Y=2.03P_Y$, $P_Y=k_0\delta_Y$, $\frac{k_1}{k_0}=\frac{\alpha_D-\mu_D}{(\mu_D-1)^n}\cdot\delta_Y^{(1-n)}=-0.443\delta_Y^{-0.371}$, $\frac{k_2}{k_0}=1+n\cdot\frac{\alpha_D-\mu_D}{\mu_D-1}=0.0325$, $n'=1+\frac{2}{n+1}\frac{\alpha_D-\mu_D}{\mu_D-1}=0.4$

Formulas (8) and (9) have been obtained from the hysteresis loops of the constant amplitude test and Formula (10) from the static test. Formula (12) has been obtained so that the line passes through the yield point $(P_Y,\delta_Y)$ and the skelton curve has the same hysteresis strain energy as in the case of the power function type until the point $(P_D,\delta_D)$ for $\mu_D=4.5$.

Earthquake Response Analysis

The elasto-plastic earthquake response analysis has been done for eight models of 8, 12, 16, 20, 24, and 28 storied buildings having the parameters in Table 5 and the distribution of mass and stiffness in Fig.9, and the natural period of $T_1=0.1N$, where N is the number of story. As the input disturbance, NS component of the El Centro Earthquake of the maximum acceleration of 300gals in 1940 was used for 9sec long. The hysteresis rule was after Jennings!(8) Maximum ductility factor has been plotted against the natural period in Fig.10. It is recognized in Fig.10 that the response for the restoring force characteristics of both bilinear and power function type are almost the same. The damage factor $\Sigma(n_i/N_i)$ of the response was calculated based on (a) Yao-Munse's, (b) Ohji-Miller's, and (c) Morrow-Landgraf's cumulative damage theories considering mean strain, and plotted in Fig.11 versus the natural period and in Fig.12 versus the ductility factor. The range-pair count method was adopted as the counting method of cycles. In Fig.12, it is recognized that different damage factors are obtained for the same ductility factor and the larger the ductility factor is, the larger the difference and that this tendency is larger for the Yao-Munse's theory than for the Ohji-Miller's. Consequently, it is concluded that the maximum ductility factor can not be a sure measure compared with the damage factor.

## CONCLUSIONS

In this study, both constant and random displacement amplitude low cycle fatigue tests were conducted for the steel frames used in tall residential buildings, and after formulating the restoring force characteristics, realistic earthquake response analyses were done for 8~28 storied buildings, and then, the random fatigue theories were applied to their results. The following conclusions have been obtained:

(1) Although in the static test, the frame attains to failure by lateral buckling of the upper girder, in all the fatigue tests, the frames do by propagation of crack initiated at the weld of the flange of the girder end and the stiffener of the panel zone.

(2) In the constant amplitude fatigue test as well as in the random fatigue test, the relationship $\overline{\Delta\delta}=aN_f^{-0.12}+bN_f^{-0.74}$ has been obtained, where $N_f$ is the number of cycles to failure, $\overline{\Delta\delta}$ the rms. interfloor displacement amplitude and a and b the constants.

(3) The damage factor in the random low cycle fatigue test due to the white noise has been found to be smaller than unity.

(4) Since, according to the earthquake response analysis, different damage factors are obtained for the same ductility factor, the maximum ductility factor can not be a sure measure.

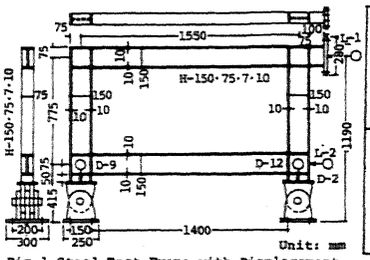


Fig.1 Steel Test Frame with Displacement Meters

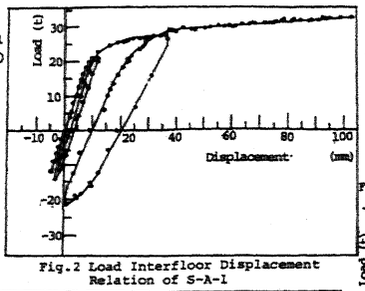


Fig.2 Load Interfloor Displacement Relation of S-A-1

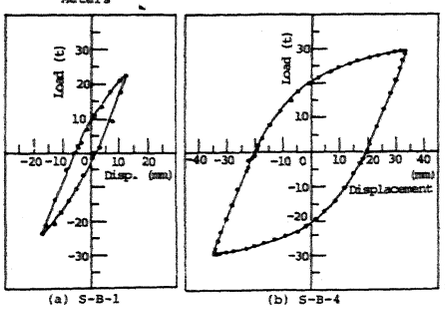


(a) S-B-1 (b) S-B-4

Fig.3 Load Interfloor Displacement Hysteresis Loops

Fig.8 Restoring Force Characteristics of Power Function and Bilinear Types

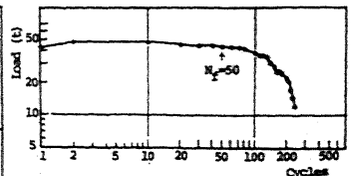


Fig.5(a) Variation of Load Range for Interfloor Displacement Cycling in S-B-1

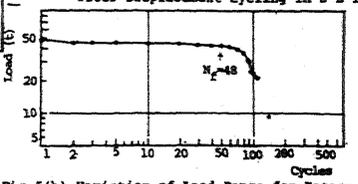


Fig.5(b) Variation of Load Range for Interfloor Displacement Cycling in S-B-2

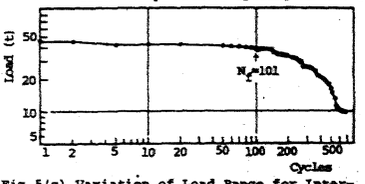


Fig.5(c) Variation of Load Range for Interfloor Displacement Cycling in S-B-3

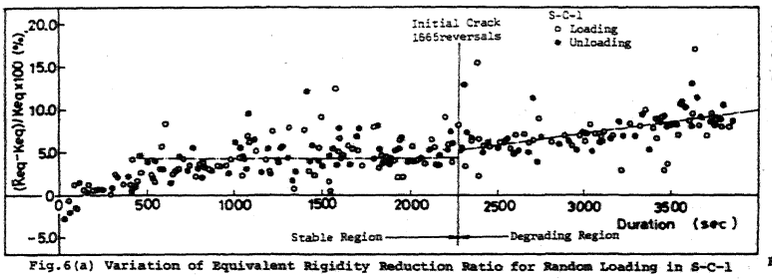


Fig.6(a) Variation of Equivalent Rigidity Reduction Ratio for Random Loading in S-C-1

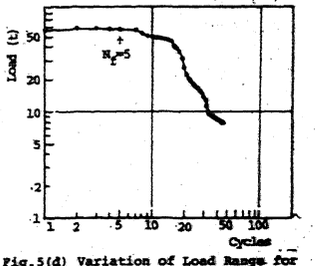


Fig.5(d) Variation of Load Range for Interfloor Displacement Cycling in S-B-4

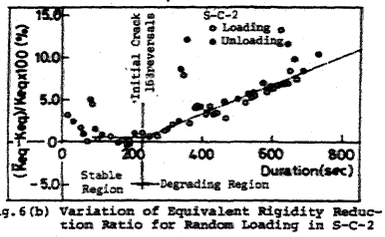


Fig.6(b) Variation of Equivalent Rigidity Reduction Ratio for Random Loading in S-C-2

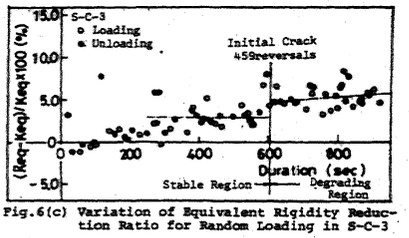


Fig.6(c) Variation of Equivalent Rigidity Reduction Ratio for Random Loading in S-C-3

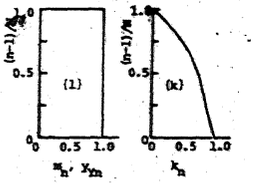


Fig.9 Distribution of Mass and Stiffness along Height

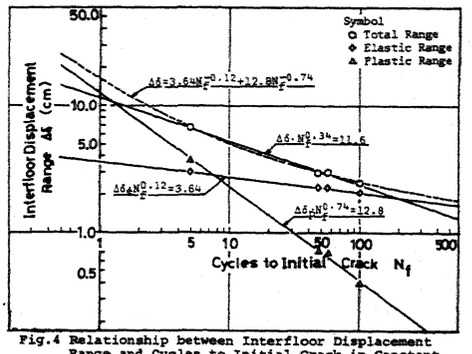


Fig.4 Relationship between Interfloor Displacement Range and Cycles to Initial Crack in Constant Amplitude Tests

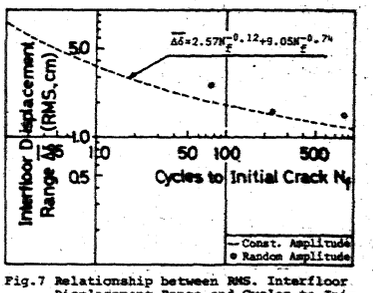


Fig.7 Relationship between RMS. Interfloor Displacement Range and Cycles to Initial Crack in Constant Amplitude and Randomly Varying Loads

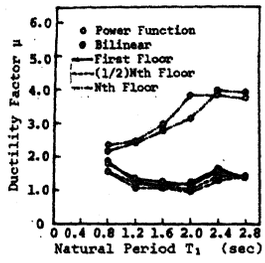


Fig.10 Relation of Maximum Ductility Factor vs. Natural Period in Earthquake Response

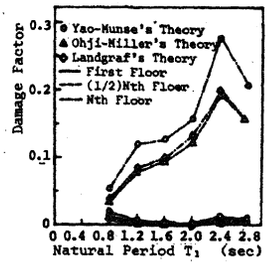


Fig.11 Relation of Damage Factor vs. Natural Period in Earthquake Response

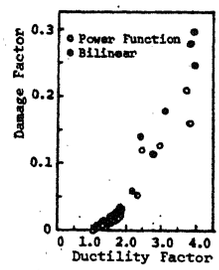


(a) Yao-Munse's Theory

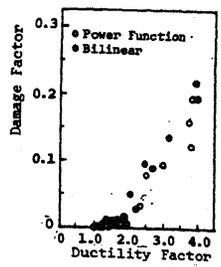


(b) Ohji-Miller's Theory

Fig.12 Relations of Damage Factor Vs. Maximum Ductility Factor in Earthquake Response

Table 1 Results of the Static Test, S-A-1

| Test Frame | S-A-1 |
|---|---|
| Load-Interfloor Displacement Curve | One linear part and one curved part (Fig.2) |
| Initial Rigidity | 26.3t/cm |
| Linear Range | (0,0)~(17t, 7mm) |
| $P=k\delta^n$ Formula | $P=16.646^{0.142}$ (2nd cycle)<br>$P=18.156^{0.134}$ (3rd cycle) |
| Maximum Load | 32.8t |
| Max. Interfloor Displacement | 10.4cm (10.4/77.5rad) |
| Strain Distribution | Maximum in the panel zone and next in the flange of the girder end |
| Mode of Fracture | Lateral buckling of the upper girder and cracking in the weld of the lower girder end |

Table 4 Fatigue Damage Factor in the Random Load Fatigue Tests

| Fatigue Damage Theory | S-C-1 | S-C-2 | S-C-3 | AV. |
|---|---|---|---|---|
| 1.Sachs-Weiss's Theory | 0.36 | 0.40 | 0.30 | 0.35 |
| 2.Yao-Munse's Theory | 0.57 | 0.42 | 0.37 | 0.45 |
| 3.Ohji-Miller's Theory | 0.34 | 0.38 | 0.28 | 0.33 |
| 4.Landgraf's Theory | 0.42 | 0.64 | 0.31 | 0.46 |

Table 2 Results of the Dynamic Constant Amplitude Fatigue Tests

| Test Frame | S-B-1 | S-B-2 | S-B-3 | S-B-4 |
|---|---|---|---|---|
| Interfloor Displacement Range ($\Delta\delta$, mm) | 29.7 | 30.6 | 25.4 | 68.0 |
| Maximum Rotation Angle of the Column (rad.) | 1/52.2 | 1/50.6 | 1/61 | 1/22.8 |
| Maximum Ductility Factor | 2.13 | 2.19 | 1.81 | 4.86 |
| Number of Cycles to Failure, $N_f$ | 50 | 48 | 101 | 5 |
| $\Delta\delta$-$N_f$ Relationship ($\Delta\delta$, mm) | $\Delta\delta \cdot N_f^{0.34}=11.6$ or $\Delta\delta=3.64N_f^{0.12}+12.8N_f^{0.74}$ | | | |
| Restoring Force Characteristics | Spindle shape | | | |
| Strain Hardening Exponent, n (Available Range, mm) | 0.659 (12.7~) | 0.732 (12.16~) | 0.760 (16.3~) | 0.620, 0.228 (13.13~, 45.2~) |
| Equivalent Rigidity (t/mm) | 1.480 | 1.448 | 1.596 | 0.843 |
| Equivalent Viscous Damping Ratio | 0.0895 | 0.074 | Unreadable | 0.299 |
| Mode of Failure | Welded Part | | | |
| Right-up corner | Left end of upper stiffener | Flange at the girder end | Left end of upper stiffener | Left end of both stiffeners and panel zone |
| Right-down corner | Lower flange at the girder end | Flange at the girder end | Flange at the girder end | None |
| Left-up corner | Right end of upper stiffener | Right end of upper stiffener | None | Right end of upper stiffeners and panel zone |
| Left-down corner | Upper flange at the girder end | Upper flange at the girder end | Upper flange at the girder end | Upper flange at the girder end |
| Concrete | | | | |
| Cyclic Rate | | 4.4sec/cycle | | 10sec/cycle |
| Control | Fair | good | good | Excellent |

Table 3 Number of Cycles to Initial Crack and Root Mean Square Displacement Amplitude in the Random Load Fatigue Tests

| | | Total Amplitude or Range (cm) | | | Plastic Amplitude or Range (cm) | | |
|---|---|---|---|---|---|---|---|
| | | S-C-1 | S-C-2 | S-C-3 | S-C-1 | S-C-2 | S-C-3 |
| Peak Count Method | 2N | 1195 | 102 | 306 | 150 | 15 | 37 |
| All Peaks Count Method | 2N | 1865 | 153 | 459 | 207 | 17 | 45 |
| Range Count Method | 2N | 1865 | 153 | 459 | 207 | 17 | 45 |
| Range-mean Count Method | 2N | 1865 | 153 | 459 | 207 | 17 | 45 |
| Range-pair Count Method | N | 833 | 77 | 226 | 104 | 9 | 23 |
| Total Range 0.2cm | N | 552 | 61 | 145 | | | |
| Full Wave Count Method | N | 833 | 77 | 226 | 104 | 9 | 23 |
| Total Range 0.2cm | N | 552 | 61 | 145 | | | |
| RMS. Displacement Amplitude | | 0.755 | 1.290 | 0.801 | | | |

Table 5 Parameters of Structures on the First Floor Used in the Earthquake Response Analysis

| | | N(Stories) | | | | | | Distribution |
|---|---|---|---|---|---|---|---|---|
| | | 8 | 12 | 16 | 20 | 24 | 28 | |
| Natural Period | $T_1$(sec) | 0.8 | 1.2 | 1.6 | 2.0 | 2.4 | 2.8 | |
| Mass | $m_1$(t·sec²/cm) | 1.0 | 1.0 | 1.0 | 1.0 | 1.0 | 1.0 | (1) |
| Rot.Angle of Column | $\phi_y$(rad) | 1/308 | 1/273 | 1/243 | 1/220 | 1/202 | 1/188 | |
| Base Shear Coef. | $C_B$ | 0.286 | 0.209 | 0.173 | 0.152 | 0.137 | 0.128 | |
| Initial Stiffness | $K_0$(t/cm) | 2226 | 2161 | 2129 | 2110 | 2097 | 2088 | (k) |
| Damping Coefficient | $C_d$(t·sec/cm) | 1.89 | 1.86 | 1.84 | 1.84 | 1.83 | 1.83 | (k) |
| Yield Displacement | $y_y$(cm) | 1.01 | 1.14 | 1.27 | 1.41 | 1.53 | 1.65 | (1) |
| Disp. for D.F.=4.5 | $y_p$(cm) | 8.49 | 8.37 | 8.31 | 8.27 | 8.24 | 8.22 | (1) |
| Load for D.F.=4.5 | $F_p$(t) | 4546 | 4985 | 5508 | 6028 | 6526 | 6999 | |


ACKNOWLEDGEMENT

The authors wish to express their sincere gratitude to the Japan Housing Corporation and the Shinnihon Steel Company for preparing the test frames. Also, assistance of Mr. Tadahiro Fukusumi, Mrs. Michiko Tanimoto, Mr. Takashi Ukita, Mr. Hiromi Matsuo and other members of the Structural Dynamics Laboratory at Kobe University in performing the experiment is greatly appreciated.


BIBLIOGRAPHY


(1) K. Mizuhata, Y. Gyoten, H. Kitamura, T. Ukita: "Study on Low Cycle Fatigue and Restoring Force Characteristics of Steel Frames and Steel-Concrete Frames", Proc. of the Fourth Japan Earthquake Engineering Symposium, 1975, pp. 943~950.
(2) Y. Gyoten, K. Mizuhata, I. Tsuyama: "Experimental Study on Low Cycle Fatigue of a Structural Member Subjected to Earthquake Loads", Proc. of the Fifth World Conference on Earthquake Engineering, 1974, pp. 1153~1156.
(3) J. Schijve: "Random Load-Time Histories with Relation to Fatigue Tests", Fatigue of Aircraft Structures, Pergamon Press, 1963.
(4) G. Sachs, V. Weiss: "Beitrage zu Kurzzeitermüdung", Zeitschrift für Metallkunde, Vol.53, 1962, pp. 37~47.
(5) J. T. P. Yao, W. H. Munse: "Low-Cycle Axial Fatigue Behavior of Mild Steel", ASTM, STP. 338, 1963, pp. 5~24.
(6) K. Ohji, W. R. Miller, J. Marin: "Cumulative Damage and Effect of Mean Strain in Low Cycle Fatigue of a 2024-T351 Aluminum Alloy", ASME Paper No. 65-WA/Met-5, 1965.
(7) R. W. Landgraf: "Cumulative Fatigue Damage under Complex Strain Histories", ASTM, STP. 519, 1973, pp. 213~228.
(8) P. C. Jennings: "Earthquake Response of a Yielding Structure", Proc. of ASCE, Vol. 91, EM4, Aug., 1965, pp. 41~68.